

UC San Diego

UC San Diego Previously Published Works

Title

Thermal Triaxial Tests to Evaluate Improvement of Soft Marine Clay through Thermal Consolidation

Permalink

<https://escholarship.org/uc/item/7t29v1j8>

Journal

Geotechnical Testing Journal, 46(3)

ISSN

0149-6115

Authors

Huancollo, Hiden Jaime Machaca
Saboya, Fernando
Tibana, Sérgio
[et al.](#)

Publication Date

2023-05-01

DOI

10.1520/gtj20220154

Peer reviewed

1
2
3 1 **Thermal triaxial tests to evaluate improvement of soft marine clay through**
4
5 2 **thermal consolidation**
6
7 3
8 4
9

10 4
11 5 **Hiden Jaime Machaca Huancollo¹, Fernando Saboya Jr.², Sérgio Tibana³, John Scott**
12 6 **McCartney⁴, Ricardo Garske Borges⁵**
13
14
15 7
16
17 8
18
19
20
21
22
23
24
25
26
27
28
29
30
31
32
33
34
35
36
37
38
39
40
41
42
43
44
45
46
47
48
49
50
51
52
53
54
55
56
57
58
59
60

1 Formerly MSc Student – State University of Norte Fluminense Darcy Ribeiro – UENF Department of Civil Engineering, Rio de Janeiro, Brazil, geomachaca@gmail.com

2 Professor - State University of Norte Fluminense Darcy Ribeiro – UENF, Department of Civil Engineering, Av. Alberto Lamego 2000 - CCT, Campos Rio de Janeiro, Brazil, CEP 28016-812, Tel +(55)22-27397369, saboya@uenf.br. ORCID **0000-0001-9063-5090**

3 Professor - State University of Norte Fluminense Darcy Ribeiro – UENF, Department of Civil Engineering, Rio de Janeiro, Brazil, stibana@gmail.com. ORCID **0000-0002-9425-8461**

4 Professor and Department Chair - University of California San Diego, Department of Structural Engineering, 9500 Gilman Dr. La Jolla, CA, USA, Tele-fax: +001-858-534-9630, mccartney@ucsd.edu. ORCID 0000-0003-2109-0378

5 Civil Engineer - Petrobras CENPES, Research and Development Center, Rio de Janeiro, Brazil, garske@petrobras.com.br. ORCID **0000-0001-7623-0337**

9 ABSTRACT

10 This paper presents an experimental study on the thermo-mechanical behavior of
11 marine clay from the Santos Basin off the coast of Brazil. The aim of the study is to assess the
12 gain in undrained shear strength of reconstituted, normally consolidated clay specimens after
13 drained thermal consolidation using a thermal triaxial device. The motivation behind
14 performing these tests is that relatively few studies in the literature have focused on
15 understanding the changes in shear strength of normally consolidated clays after a heating-
16 cooling cycle, a path encountered in using heat to improve the properties of soft clays. Further,
17 the high plasticity marine clays evaluated in this study have a pronounced thermal creep
18 different from that observed in previous nonisothermal tests on clays. Isotropic, consolidated
19 undrained (CIU) triaxial compression tests were performed on specimens consolidated to
20 effective stresses of 100, 200 and 400 kPa then sheared conventionally at room temperature as
21 well as after drained heating-cooling cycles with maximum temperatures of 40 and 55 °C. The
22 results were analyzed according to critical state soil mechanics after drained thermal
23 consolidation, which was well suited to explain the improvement in undrained shear strength.
24 The results have potential implications on the development of techniques that can promote
25 thermal improvement of deep-water offshore anchors installed in soft soil.

26 **Keywords:** Thermal consolidation, thermal creep, shear strength, marine clay.

27 INTRODUCTION

28 Early studies on the effects of temperature on soil properties from the 1960's focused
29 on understanding sampling effects associated with extracting soils from the cold subsurface to
30 the warm ground surface and the impacts of buried electrical cables (e.g., Campanella &
31 Mitchell 1968, Plum & Esrig 1969). These studies led to a basic understanding of undrained
32 thermal loading and drained thermal consolidation, as well as establishing the temperature
33 effects on soil properties like the compression indices and strength envelope. With the

1
2
3 34 popularization of nuclear energy, concerns arose regarding encapsulation of radioactive waste
4
5 35 in low permeability clays reactivated the interest in understanding the influence of temperature
6
7 36 on the mechanical properties of both soft and compacted soils (e.g., Houston *et al.* 1985;
8
9 37 Hueckel & Baldi 1990; De Bruyn & Thimus 1996; Delage *et al.* 2000). In recent years,
10
11 38 geotechnical studies have focused on the mechanical behavior and thermal response of buried
12
13 39 energy geostructures under elevated temperatures, with thermal piles being the most popular
14
15 40 (e.g., Brandl 2006; Laloui *et al.* 2006; Bourne-Webb *et al.* 2009, Laloui *et al.* 2014). Several
16
17 41 recent studies have found that the heating and cooling operations of thermal piles may have
18
19 42 effects on the thermo-mechanical behavior of the surrounding soil, which, in turn, can influence
20
21 43 the mechanisms of soil-structure interaction or axial capacity of the thermal pile (e.g., Ng *et al.*
22
23 44 2014, 2021; Goode & McCartney 2015; McCartney & Murphy 2017; Ghaaowd & McCartney
24
25 45 2018, Ghaaowd *et al.* 2018, 2021; Yazdani *et al.* 2019a, 2019b, 2021).

26
27 46 To explain the phenomena observed in different applications mentioned above, several
28
29 47 fundamental experimental studies have investigated the effects in the mechanical properties of
30
31 48 soils under variation in temperature on saturated soils with different stress histories (e.g.,
32
33 49 Houston *et al.* 1985; Hueckel & Baldi 1990; Kuntiwattanakul *et al.* 1995; Burghignoli *et al.*
34
35 50 2000; Cekerevac & Laloui 2004; Cekerevac & Laloui 2010; Bai *et al.* 2014; Di Donna & Laloui
36
37 51 2015; Vryzas *et al.* 2017; Samarakoon *et al.* 2018; Samarakoon & McCartney 2020; Rotta
38
39 52 Loria & Coulibaly 2021). Some few studies are focused specifically on unsaturated conditions
40
41 53 (Uchaipichat & Khalili 2009; Coccia & McCartney 2016). The volume change of fine-grained
42
43 54 soils due to heating, has been carefully studied and the results have built a strong basis for the
44
45 55 development of constitutive models that describe the thermal volumetric strains (e.g., Cui *et*
46
47 56 *al.* 2000; Laloui & Francois 2009; Di Donna & Laloui 2015; Coccia & McCartney 2016; Hong
48
49 57 *et al.* 2016; Hong *et al.* 2013, Zhou & Ng 2018; Cheng *et al.* 2020). The mechanisms of volume
50
51 58 change under heating from these studies, which include both thermal consolidation and thermal
52
53
54
55
56
57
58
59
60

1
2
3 59 creep have helped explain the effects of stress history, degree of saturation, viscosity, and other
4
5 60 variables (Abuel-Naga *et al.*, 2007a; Graham *et al.* 2001; Hueckel *et al.* 2009; Tsutsumi and
6
7 61 Tanaka 2012; Coccia & McCartney 2016; Li *et al.* 2018; Rotta Loria & Coulibaly 2021; Zeinali
8
9 62 and Abdelaziz 2021). Most past studies in the literature focused predominantly on
10
11 63 overconsolidated soils (often with a single normally consolidated specimen for comparison),
12
13 64 and usually focus on the shear strength of soils under elevated temperatures, with only a few
14
15 65 focused on understanding the change in shear strength after a heating-cooling cycle
16
17 66 (Samarakoon *et al.* 2018; Jaradat and Abdelaziz 2019). Accordingly, a goal of this study is to
18
19 67 better understand the behavior of normally consolidated clays after a heating-cooling cycle in
20
21 68 a similar manner as shown by Abuel-Naga *et al.* (2007b).

22
23
24
25
26 69 Despite the wealth of data generated in the aforementioned studies, heating of soils with
27
28 70 the goal of modifying their behavior has not been fully explored in engineering practice in the
29
30 71 face of its great potential as a soil improvement technique. While there are many soil
31
32 72 improvement techniques used in geotechnical practice, ranging from chemical additives,
33
34 73 installation of mechanical inclusions such as stone columns, application of a surcharge with
35
36 74 vertical drains, to compaction, these techniques are best suited for onshore situations and
37
38 75 cannot be readily applied to soft soils under the sea floor in deep water environments. In this
39
40 76 scenario, thermal consolidation may be an attractive alternative for offshore industry. Thermal
41
42 77 consolidation has been successfully deployed for soil improvement using geothermal heat
43
44 78 exchangers (Bergentahl *et al.* 1994), thermal drains (Abuel-Naga *et al.* 2006; Pothiraksanon
45
46 79 *et al.* 2010; Artidteang *et al.* 2011; Salager *et al.* 2012; Salager *et al.* 2010), and thermal piles
47
48 80 (Ghaaowd *et al.* 2018, 2021; Ghaaowd & McCartney 2018) in saturated soil deposits. However,
49
50 81 questions remain regarding predictions of the change in undrained shear strength after a
51
52 82 heating-cooling cycle, especially those related to the mechanical response after thermal
53
54 83 consolidation.
55
56
57
58
59
60

1
2
3 84 Herein, a set of thermal triaxial tests was carried out on remolded marine clay
4
5 85 specimens from southern of Brazil to quantify the impact of thermal consolidation and thermal
6
7 86 creep associated with a heating-cooling cycle with the goal of understanding the improvement
8
9 87 in shear strength response under undrained shearing. This new understanding will help
10
11 88 establish a geotechnical approach based on thermal triaxial testing to quantify the expected
12
13 89 thermal improvement associated with enhancing the staying capacity of offshore anchors like
14
15 90 torpedo piles, which are extensively used in Brazil for anchoring heavy floating oil exploration
16
17 91 platforms in deep waters. The test results were interpreted considering the critical state soil
18
19 92 mechanics framework with the aid of thermal consolidation modeling approaches.
20
21
22
23

24 93 **BACKGROUND**

25
26 94 Studies on normally consolidated clays employing thermal oedometer and triaxial tests
27
28 95 by Campanella & Mitchell (1968), Plum & Esrig (1969), Burghignoli *et al.* (2000), and Laloui
29
30 96 & Cekerevac (2003) observed that additional volumetric strains on the order of 1-2% can be
31
32 97 encountered when heating normally consolidated (NC) clayey soil specimens under constant
33
34 98 mechanical loading to temperatures of approximately 60-80 °C. Primary thermal consolidation
35
36 99 is the result of compression caused by the dissipation of thermally induced pore pressures,
37
38 100 along with secondary thermal consolidation resulting from the compression due to the
39
40 101 rearrangement of interparticle forces and fabric structural changes at elevated temperature.
41
42 102 Campanella & Mitchell (1968) predicted changes in total volume ($(\Delta V_m)_{\Delta T}$) and pore water
43
44 103 pressure (Δu) caused by an increase in temperature using the coefficients of thermal expansion
45
46 104 of minerals and water and the coefficient of compressibility m_v of the soil skeleton. As for the
47
48 105 compression index (C_c) and recompression index (C_e) deduced from oedometer tests in the \log
49
50 106 (σ_v) $\times e$ plane and the well-known parameters λ and k in the $\ln(p) \times e$ plane, authors such as
51
52 107 Campanella & Mitchell (1968), Plum and Esrig (1969), Burghignoli *et al.* (2000) and Laloui
53
54
55
56
57
58
59
60

1
2
3 108 & Cekerevac (2003) observed that they are independent of temperature for heated-cooled
4
5 109 specimens.

6
7
8 110 Several studies have noted that the stress history can play an important role in thermal
9
10 111 volume change. For over-consolidated (OC) soils, Baldi *et al.* (1988) found that a rise in
11
12 112 temperature has a thermal-elastic effect (dilation) and that slightly overconsolidated and
13
14 113 normally consolidated (NC) soils tend to present a contractive behavior with irreversible
15
16 114 volumetric strains. The latter feature is important for thermal improvement, where the soils
17
18 115 under the seabed are expected to be normally consolidated. In the case of a soil specimen
19
20 116 subjected to more than one heating-cooling cycle, Campanella & Mitchell (1968), Vega &
21
22 117 McCartney (2015), Di Donna & Laloui (2015), Burghignoli & Desideri (1988) and Plum &
23
24 118 Esrig (1969) concluded that the effects on volume change is more pronounced during the first
25
26 119 heating, because, after cooling the soil tends to exhibit over-consolidated behavior and a stiffer
27
28 120 response. Studies like Jaradat and Abdelaziz (2019) noted the importance of controlling the
29
30 121 rate of cooling in addition to the rate of heating.

31
32
33 122 When a normally consolidated saturated clay is heated under constant isotropic
34
35 123 effective stress in undrained conditions, differential expansion of the pore water and soil solids
36
37 124 leads to excess pore water pressures. If drainage is allowed, these excess pore water pressures
38
39 125 will dissipate resulting in a time-dependent volume change Campanella & Mitchell (1968).
40
41 126 This is referred to as thermal consolidation, and theories for the time dependency have been
42
43 127 developed (e.g., Zeinali & Abdelaziz 2021). Houston *et al.* (1985) found that the higher the
44
45 128 increase in temperature, the greater the excess pore water pressure generated during undrained
46
47 129 heating, which may decrease the effective stress to the point of shear failure.

48
49
50 130 To account for the thermal volume change of soils with different stress histories, several
51
52 131 thermo-elastoplastic models have been proposed. Hueckel & Baldi (1990) and Laloui &
53
54 132 François (2009) proposed thermoplastic models for normally and over consolidated saturated
55
56
57
58
59
60

1
2
3 133 clays. Cui *et al.* (2000) have developed a dedicated thermo-elastoplastic model, while Graham
4
5 134 *et al.* (2001) and Abuel-Naga *et al.* (2009) proposed a modified Cam-Clay model considering
6
7
8 135 the effects of temperature. Coccia & McCartney (2016) presented an alternative constitutive
9
10 136 model using the secondary compression to model the thermal volumetric change where the
11
12 137 water viscosity at different temperatures plays an important role in this process. They noted
13
14 138 that the thermal volume change is associated with the prior mechanical loading path through
15
16 139 thermally accelerated creep, and that an overconsolidated clay may show thermal expansion or
17
18 140 contraction depending on whether it was previously loaded or unloaded. Most of these
19
20 141 approaches indicate that both thermal consolidation and thermal creep mechanisms may come
21
22 142 into play during thermal volume changes.

23
24
25 143 Drainage of thermally induced excess pore water pressures (primary thermal
26
27 144 consolidation) and thermal creep (secondary thermal consolidation) lead to a densification of
28
29 145 normally consolidated clays and an increase in undrained shear strength, which is the main goal
30
31 146 of thermal improvement. Some of the studies whose objective was to assess the influence of
32
33 147 temperature on the shear strength of clays are summarized in Table 1. Most of the authors
34
35 148 observed a rise in shear strength in normally consolidated (NC) clays heated under drained (D)
36
37 149 and sheared in undrained conditions. In the case of over-consolidated (OC) clays, some authors
38
39 150 in Table 1 stated that shear strength is not strongly dependent of the temperature. Houston *et*
40
41 151 *al.* (1985) performed undrained triaxial tests at temperatures of up to 180 °C and found that the
42
43 152 thermal consolidation of soils leads to an enhancement in undrained shear strength like that
44
45 153 obtained from mechanical consolidation. Burghignoli *et al.* (2000) studied the influence of
46
47 154 thermal history on shear strength using triaxial tests, denominating “normally heated” (NH) for
48
49 155 specimens that were never exposed to temperatures above the current temperature and
50
51 156 “overheated” (OH) for specimens subjected to temperatures above the current temperature. The
52
53 157 authors reported that the peak deviatoric stress of OH specimens are an average of 10% higher
54
55
56
57
58
59
60

1
2
3 158 than those of NH. This change seems to indicate that thermal history may have an influence on
4
5 159 the critical state line of clays. However, authors such as Houston *et al.* (1985), Abuel-Naga *et*
6
7 160 *al.* (2007a), Cekerevac *et al.* (2005) and Hamidi *et al.* (2017) concluded that the slope of the
8
9 161 critical state line is independent of temperature. On the other hand, Abuel-Naga *et al.* (2007a)
10
11 162 indicated that this may not always be the case for natural soils due to difficulty in obtaining
12
13 163 identical undisturbed subsoil samples.
14

15
16
17 164 Abuel-Naga *et al.* (2007a) and Cekerevac *et al.* (2005) observed that the ratio between
18
19 165 volumetric and shear plastic strain ($d\varepsilon_v^p/d\varepsilon_s^p$) increases with temperature. This behavior
20
21 166 suggests that the plastic flow rule depends on temperature. Abuel-Naga *et al.* (2007a) also state
22
23 167 that the Roscoe surface is steeper with increasing temperature and proposed a
24
25 168 thermomechanical model for saturated clays to capture this feature.
26
27

28 169 **MATERIALS**

29
30
31 170 The marine clay used in this study was sampled from the seabed off the coast of Brazil
32
33 171 at a depth of 0.70 m from the sea floor under a water depth of 3,000 m. The main physical
34
35 172 properties of marine clay are depicted in Table 2. It can be characterized as a very fine material,
36
37 173 containing 2.4% fine sand, 27.5% silt and 70.1% clay. The fines fraction exhibits high plasticity
38
39 174 with an elevated colloidal activity of 0.93. The clay classifies as CH according to the Unified
40
41 175 Soil Classification System (USCS).
42
43

44
45 176 The triaxial tests performed as part of this study were conducted on reconstituted clay
46
47 177 specimens due to the limited number of intact samples obtained from the field. After removing
48
49 178 and homogenizing the clay from the Shelby tubes, it was then reconstituted in a wet chamber
50
51 179 to maintain the original gravimetric water content constant with salt water as the porous fluid.
52
53 180 The saturation degree at the end of reconstitution was about 95%. Afterwards, the clay was
54
55 181 consolidated one-dimensionally inside a cylindrical mold in K_0 conditions using a hydraulic
56
57 182 actuator to reach a vertical effective stress of 100 kPa. This process lasted five days and the
58
59
60

1
2
3 183 load was applied in five steps up to desired vertical effective stress. After that, the specimens
4
5 184 were then trimmed to an $H/D=2$ ratio (Height H of 76.2 mm; Diameter D of 38.0 mm) for
6
7 185 triaxial testing. After being unloaded during extraction from the cylindrical mold and
8
9 186 recompressed isotropically inside the triaxial cell to a minimum effective cell pressure of
10
11 187 100 kPa, the clay specimens were assumed to be normally consolidated as the mean effective
12
13 188 stress in the triaxial cell is greater than the mean effective stress in the cylindrical mold under
14
15 189 K_0 conditions.
16
17
18

19 190 **THERMAL TRIAXIAL TEST DEVICE AND METHODS**

21 191 The experimental program was carried out in a customized thermal triaxial cell
22
23 192 manufactured by GDS Instruments. The insulated aluminum chamber allows heating to a
24
25 193 maximum temperature of 65 °C under a maximum cell pressure of 4 MPa. A schematic diagram
26
27 194 of the triaxial chamber is shown in Figure 1 with all the instruments installed, including three
28
29 195 thermocouples, one displacement transducer, one load cell, one pore pressure transducer, two
30
31 196 thermal pads attached to the outside of the aluminum cell, and a back-pressure control system.
32
33 197 The sensors incorporated into the thermal triaxial cell were selected to have a stable response
34
35 198 within the temperature ranges investigated in this study. Heat is transferred to the test specimen
36
37 199 by heating the water inside the cell using computer controlled electrical resistor coils. The
38
39 200 volume change and the vertical strain during the heating phase were measured using,
40
41 201 respectively, the cell fluid volume and, a servo-controlled device that allowed keeping the
42
43 202 vertical load cell always in contact with the top of the soil specimen without delivering any
44
45 203 extra load during the heating-cooling process.
46
47
48
49

51 204 The conventional triaxial tests at room temperature, to serve as reference tests for the
52
53 205 subsequent tests, were performed following the procedures in ASTM D4767-11(2020) for
54
55 206 consolidated isotropic undrained (CIU) triaxial testing. Filter paper strips were used to promote
56
57 207 drainage across the specimens. All triaxial tests were performed under back-pressure to ensure
58
59
60

1
2
3 208 that the specimen was saturated ($B=0.98$ minimum) and involved mechanical consolidation to
4
5 209 the target initial effective stress before shearing in constant strain rate of 0.06mm/min. For the
6
7 210 thermal triaxial tests, thermal consolidation during heating and uncontrolled natural cooling
8
9 211 stages were added after primary mechanical consolidation was achieved, as shown in Figure 2.
10
11
12 212 The characteristics of the thermal additional stages are described in Figure 2, which comprise:

13
14 213 i. Drained thermal consolidation: this additional stage consists of raising the temperature
15
16 214 of the specimen up to " T_f " (Fig. 2) under constant hydrostatic stress at a heating rate of
17
18 215 0.5 °C/min while the drainage valves at the top and bottom of the specimen were kept
19
20 216 open to ensure double drainage. The excess of pore pressure during heating was
21
22 217 monitored using the pressure sensor attached to the pressure-volume controllers to
23
24 218 ensure that it was negligible during drained heating. This stage lasted 24 hours
25
26 219 following a common practice adopted during conventional creep oedometer tests on
27
28 220 this soil, with the goal of capturing both the primary and secondary thermal
29
30 221 consolidation stages in a consistent manner in each test for ease of comparison. Primary
31
32 222 thermal consolidation was observed to occur in only a few hours after reaching a stable
33
34 223 temperature, while secondary thermal consolidation was not observed to stabilize.
35
36 224 Longer periods of heating will undoubtedly lead to additional creep and further
37
38 225 decreases in volume, but the goal of this study was to characterize the changes in soil
39
40 226 behavior.

41
42 227 ii. Cooling: consists of reducing the temperature from T_f reached in the previous stage to
43
44 228 room temperature (T_r) while keeping constant the confining stress. The equipment does
45
46 229 not allow a controlled cooling and this phase consisted only of turning off the heater.
47
48 230 Accordingly, natural cooling required approximately 12 hours for stabilization of both
49
50 231 temperature and volume change at room temperature. The excess pore pressure was not
51
52
53
54
55
56
57
58
59
60

232 monitored during the cooling phase. However, based on the time required for
233 stabilization it is believed that the cooling phase was also a drained process.

234 The effect of thermal consolidation on the undrained shear strength of marine clay was
235 experimentally assessed by using two sets of testing. The first set involved reference tests that
236 consisted of standard CIU triaxial tests under confining effective stresses of 100, 200 and 400
237 kPa at a controlled room temperature of 23 ± 1 °C. The second set of tests was carried out on
238 specimens with nearly identical initial conditions to those in the conventional room temperature
239 tests (similar initial void ratio and same initial effective confining stress prior to heating),
240 consisted of undrained shearing after 24 hours of thermal consolidation of the specimens under
241 the same confining stresses of the first set. This makes possible direct comparisons between
242 the two sets of tests and, therefore, to quantify possible improvements and substantial
243 differences in mechanical response between them. An additional test, S4, was also carried out
244 in a conventional triaxial test to characterize the Unload-Reload Line (URL) in the compression
245 plane. The experimental testing program involved ten triaxial tests whose details are presented
246 in Table 3. The tests included conventional consolidated-undrained triaxial tests labelled S1
247 through S3 as well as consolidated-undrained tests after a heating-cooling cycle. These
248 included tests S6, S7 and S8 which were heated up to 40 °C and tests S9, S10 and S11 which
249 were heated up to 55 °C.

250 RESULTS

251 Thermal Consolidation

252 In this section, the results of the thermal consolidation changes of the heated tests are
253 presented, and then the stress-strain response and stress paths from consolidated undrained tests
254 are presented in the next section. It is important to mention that tests S6 to S11 involved heating
255 just after the end of isotropic mechanical primary consolidation. During each stage of
256 consolidation (i.e., mechanical consolidation; drained thermal consolidation and drained

1
2
3 257 cooling), all specimens experienced volumetric strain variation due to changes in void ratio
4
5 258 and negligible excess of pore pressure during the second stage. During cooling, the time taken
6
7 259 to the chamber to return to the room temperature probably allowed a drained process. The
8
9 260 change in void ratio for heating and cooling phases in Figure 3 shows a partial elastic rebound
10
11 261 due to cooling. The evolutions in void ratio for the tests at 40 and 55 °C during heating only,
12
13 262 normalized by the initial void ratios of each specimen, are plotted against confining stresses in
14
15 263 Figure 4. The results indicate that the higher the temperature, the greater the thermal volumetric
16
17 264 strains, as expected. After 24 hours of thermal consolidation, the deformations did not show
18
19 265 any tendency of stabilization. However, for the specimens heated to 40°C this was even less
20
21 266 evident than of specimens heated up to 55°C. On the other hand, the confining stress level does
22
23 267 not affect the thermal consolidation process. This reflects a dominant influence of the
24
25 268 temperature in the void ratio change, irrespective the initial void ratio achieved at the end of
26
27 269 primary mechanical consolidation.

28
29
30
31
32
33 270 Under constant effective confining stress, thermal consolidation caused a decrease in
34
35 271 the void ratio in the specimens. However, this change takes place in two different ways as
36
37 272 depicted in Figure 5. During transient heating the specimen experiences some volume decrease
38
39 273 of about 0.3 and 1.0% for 40 and 55°C respectively. However, besides the plastic volume
40
41 274 change recorded during constant temperature, the volume decrease during the transient phase
42
43 275 of heating is fully recovered during cooling and the slope of volume change vs. transient
44
45 276 temperature curve is not dependent on effective confining pressure nor temperature. A linear
46
47 277 trend fitted to the data indicates that a constant transient thermal volumetric variation
48
49 278 coefficient of 0.043 %/°C is encountered during the heating and cooling processes. This slope
50
51 279 reflects the tendency of the clay to change in volume under a specific heating rate before the
52
53 280 permanent heating compression takes place under stress and temperature constant. It is quite
54
55 281 useful for assessing the final void ratio after heating-cooling process. Further studies are needed
56
57
58
59
60

282 to investigate the factors influencing this slope (elastic thermal volume change during transient
283 heating).

284 For both tests, the relative volume change is not dependent on the temperature during
285 thermal consolidation, at least for the temperature ranges tested herein, and both curves show
286 the same pattern keeping a constant difference in volume change from each other. The thermal
287 volume change has greater variation when the confining stress is in the interval of 100 to 200
288 kPa irrespective of the temperature used during thermal consolidation. From test S6 onwards
289 all further tests followed the same procedures to obtain void ratios e_{f1} (after primary mechanical
290 consolidation), e_{f2} (after heating) and e_{f3} (after cooling) and are presented in Table 4.

291 **Stress Strain Response and Shear Strength Parameters**

292 The deviator stress (σ_d) and excess pore water pressure (Δu) vs. axial strain ($\epsilon_1\%$) curves
293 from all triaxial tests are shown in Figure 6. The results from conventional tests at room
294 temperature allow definition of a peak failure envelope with a slope $M=1.07$ corresponding to
295 an effective internal peak friction angle (ϕ') of 26.7° ; the slopes of the virgin compression and
296 recompression line were $\lambda=0.26$ and $\kappa=0.074$, respectively. The deviator stress (σ_d) and change
297 in pore water pressure (Δu) plotted as a function of axial strain ($\epsilon_1\%$) from all the thermal
298 triaxial tests in Figure 6 show a considerable increase in undrained shear strength of 88% and
299 98% for the specimens thermally consolidated at 40°C and 55°C , respectively. However, in
300 relation to the pore pressures generated during shear, there were no significant changes.

301 **ANALYSIS**

302 The effective stress paths from these tests are shown in Figure 7 along with the isotropic
303 compression line (LIC), the critical state line (CSL), and the equivalent time compression lines
304 according to the data obtained. The lasts are defined as the lines parallel to the LIC but
305 considering the void ratio after thermal consolidation. At first glance, these results may
306 mistakenly be interpreted that the increase in temperature generated a new failure envelope.

1
2
3 307 However, the specimens subjected to a heating-cooling cycle have lower void ratios (state
4
5 308 parameters) than the unheated specimens. The corresponding void ratios for the thermal triaxial
6
7 309 tests after cooling are the $e_{f\beta}$ whose line in the compression plane is located below the LIC at
8
9
10 310 room temperature as shown in Figures 7(b) and 7(c). For this reason, the effective stress paths
11
12 311 of the thermally consolidated specimens showed an increase in mean effective stress ($+\Delta p'$) at
13
14 312 the beginning of shearing closely following the total stress path up to vertical strains of about
15
16
17 313 1%, which correspond to approximately 60% of mobilized strength, when considerable
18
19 314 positive pore water pressures started being generated until the point of failure.

21 315 An important feature that the heating-cooling cycle reveals is the strain-rate effects in
22
23 316 the shape of the effective stress path for specimens thermally consolidated. Generally, the
24
25 317 principle of effective stress does not consider both the viscous and friction effects separately
26
27 318 because under the conventional strain-rate adopted in typical laboratory tests they occur
28
29 319 simultaneously for fine soils. However, in case of thermally consolidated soils, the viscous
30
31 320 contacts tend to disappear, and the solid-solid grain contacts prevail. During the initial stage of
32
33 321 shearing, the absence of viscous contacts will require the specimens to undergo additional shear
34
35 322 strain before pore-pressure generation occurs. Until there, the effective stress path will coincide
36
37 323 with the total stress path and the samples will show higher initial stiffness, as observed herein.
38
39 324 This is clearly observed in the zoomed detached area of the Figure 7.

44 325 A high gain in undrained strength is achieved when the specimens are thermally
45
46 326 consolidated up to 40°C ($\Delta T = 17^\circ\text{C}$) when compared with tests on specimens performed at
47
48 327 room temperature. For specimens thermally consolidated up to 55°C ($\Delta T = 32^\circ\text{C}$) there is a
49
50 328 smaller gain in undrained shear strength when compared to those thermally consolidated at
51
52 329 40°C, as shown in Figure 8. Additionally, the overall gain in undrained shear strength becomes
53
54 330 more evident with higher confining stresses. This behavior may be associated with the new soil
55
56 331 structure achieved after thermal consolidation, as mentioned above, where no pore-pressure is
57
58
59
60

1
2
3 332 generated up to 1% of vertical strain. This finding is consistent with those reported by Coccia
4
5 333 & McCartney (2016). It is well known that the cooling stage shows a significant influence on
6
7 334 the thermal hardening process of the clay, as discussed by Coccia & McCartney (2016) where
8
9
10 335 the kinematic viscosity of the adsorbed water plays a major role, along with the recent stress
11
12 336 history of the soil.

13
14 337 On the other hand, the stiffness of the clay specimens is highly impacted by thermal
15
16 338 consolidation, which is more evident for those subjected to higher confining stresses once they
17
18 339 seem to play major role in the newly formed fabric after heating, as shown in Figure 9. It is
19
20 340 known that during undrained shearing in a conventional triaxial test, the viscous strength is
21
22 341 instantaneously and fully mobilized as it depends on the strain rate only. Due to its lower
23
24 342 compressibility, the free water is loaded first and the pore water pressure is generated at low
25
26 343 levels of deformation. This mechanism is closely related to the presence of bonded water films
27
28 344 covering the soil particles as stated by Taylor (1942). Thermal consolidation seems to cause
29
30 345 more effective grain to grain contacts, as explained before. For specimens consolidated at 400
31
32 346 kPa and subjected to thermal consolidation under temperatures up to 55 °C ($\Delta T=32^{\circ}\text{C}$) the
33
34 347 stiffness can reach values of five times the stiffness at room temperature. Moreover, this
35
36 348 considerable change in stiffness also takes place for the other specimens consolidated under
37
38 349 lower confining stress, however with less intensity. This culminates in less pore water pressure
39
40 350 being generated at the beginning of the shearing process.

41
42 351 According to the results from the triaxial tests, the void ratio for clay specimens at the
43
44 352 end of thermal consolidation is somewhat smaller than that of clay specimens consolidated to
45
46 353 the same conditions at room temperature as shown in Figures 7(b) and 7(c). However, during
47
48 354 the cooling phase this difference may decrease, but this is not reflected in the strength
49
50 355 properties. This situation could also be represented within the critical state framework using
51
52 356 the concept of equivalent initial pressure.
53
54
55
56
57
58
59
60

1
2
3 357 Considering that the undrained shear strength, s_u , can be defined by:

$$4 \quad 5 \quad 6 \quad 7 \quad 8 \quad 358 \quad s_u = \frac{M}{2} \cdot \frac{p'_i}{2^\Lambda} \quad (1)$$

9 359 where M is the slope of the peak failure envelope and $\Lambda = \frac{\lambda-k}{\lambda}$. Once s_u is obtained from the
10
11 360 triaxial tests on a heated specimen, it is possible to use Eq.1 to define the equivalent initial
12
13 361 effective isotropic confining stress, p'_{ieq} . This approach was followed using the undrained shear
14
15 362 strengths for each test and the equivalent initial effective isotropic confining stresses are
16
17 363 summarized in Table 5. Therefore, a value of p'_{ct} can be defined as the isotropic pressure where
18
19 364 the value of void ratio on the isotropic compression line coincides with the void ratio reached
20
21 365 at the end of thermal consolidation under a given consolidation pressure. This procedure
22
23 366 defines a so-called pseudo/equivalent consolidation stress " p'_{ct} " caused by heating only, as
24
25 367 depicted in Figure 10, as similarly proposed by Abuel-Naga *et al.* (2007b). As the result, the
26
27 368 undrained strength defined by the shifted effective stress path will match the critical state line,
28
29 369 which in turn is not affected by the heating, as shown in Figure 11. Consequently, by using the
30
31 370 same value of undrained strength for the shifted effective stress path for each test and using the
32
33 371 Cam-Clay relationship in Equation (1) to assess the equivalent initial confining effective stress,
34
35 372 p'_{ieq} as listed in Table 5, comparison between both effective stress-paths can be done. The
36
37 373 Figure 12 shows that the effective stress paths predicted from the Cam-Clay model is somewhat
38
39 374 different in shape from those obtained from the thermal triaxial tests, although the undrained
40
41 375 strengths are the same. This indicates that the decrease in void ratio, due to the increase in
42
43 376 temperature, is not the only reason for the observed increase in undrained shear strength and
44
45 377 the resulting soil structure plays an important role in the undrained mechanical response of
46
47 378 thermally consolidated soils.

48 379 CONCLUSIONS

49 380 This study presented a detailed evaluation of the thermal improvement process of soft,
50
51 381 high plasticity clays that may be gained during a drained heating-cooling cycle under different

1
2
3 382 effective confining stresses. A clear decrease in void ratio was noted after the heating-cooling
4
5 383 cycle due to a combination of primary and secondary thermal consolidation, with greater
6
7 384 changes for higher changes in temperature and higher initial effective confining stresses. The
8
9 385 results suggest that the thermally consolidated clay specimens behave as very stiff body until
10
11 386 1% of vertical strain is reached and after which an increase in pore pressure occurs. The
12
13 387 definitions of the normally consolidated line and isotropic thermal consolidation lines were
14
15 388 necessary to numerically define the equivalent consolidation stress p'_{ct} values and to adjust the
16
17 389 effective stress path for the thermally consolidated sample, which fits well in the critical state
18
19 390 line that, in turn, is not affected by the temperature change. However, the shape of the effective
20
21 391 stress path followed by the thermally consolidated specimens is quite different from those
22
23 392 defined by the Cam-Clay model, as this model does not consider strain-rate effects which seems
24
25 393 to be critical in thermally consolidated fine soils.

26
27 394 Application of a heating-cooling cycle to the clay specimens with maximum
28
29 395 temperatures of 40 and 55 °C was found to result in 88% and 98% increases in undrained shear
30
31 396 strength, respectively, when compared to the same tests consolidated at room temperature. No
32
33 397 significant difference in the rate of volume change for both temperatures tested was found and
34
35 398 this reflects in the low difference among the undrained strength for specimens consolidated
36
37 399 under 40 and 55 °C. This is believed to result from the fact that the water viscosity does not
38
39 400 change significantly for temperatures greater than 40 °C above which the rate in water viscosity
40
41 401 variation falls from 0.02 to 0.005 mPa.s/°C. At the same time, the major change in soil structure
42
43 402 takes place up to 40 °C.

44
45 403 This study provides unique insight into the thermo-mechanical response of high
46
47 404 plasticity soft clays that can experience significant thermal creep after the end of primary
48
49 405 thermal consolidation. From a practical perspective, the results of this study may have
50
51 406 promising implication in using thermal consolidation of soft clays to improve the pullout
52
53
54
55
56
57
58
59
60

1
2
3 407 capacity of deep water anchors like torpedo piles embedded in the clay, with the heating
4
5 408 element installed within the pile. The water temperature off the coast of Brazil, in deep water,
6
7 409 is somewhat constant around 4 °C and small changes in temperature will make water viscosity
8
9 410 vary considerably which may help promote the clay thermal consolidation process.

411 **ACKNOWLEDGEMENTS**

412 This study was partially supported by Petrobras (Brazilian Petroleum Company) Grant
413 No TC 0050.0–98204.15.9 - SAP 4600499688. We also thank the Brazilian Scholarship
414 Agency – CAPES for supporting the first author. The last author was supported by NSF CMMI
415 grant 1941571. The opinions in this paper are those of the authors alone.

416 **REFERENCES**

- 417 Abuel-Naga, H.M., Bergado, D.T., & Chaiprakaikeow, S. (2006). Innovative thermal
418 technique for enhancing the performance of prefabricated vertical drain during the
419 preloading process. *Geotextiles and Geomembranes*, 24, 359–370.
- 420 Abuel-Naga, H.M., Bergado, D.T., & Lim, B.F. (2007a). Effect of temperature on shear
421 strength and yielding behavior of soft Bangkok clay. *Soils and Foundations*, 47(3),
422 423-436.
- 423 Abuel-Naga, H.M., Bergado, D.T., Bouazza, A., & Pender, M. (2009). Thermomechanical
424 model for saturated clays. *Géotechnique*, 59(3), 273-278.
- 425 Abuel-Naga, H. M., Bergado, D. T., Bouazza, A., & Ramana, G. V. (2007b). Volume change
426 behaviour of saturated clays under drained heating conditions: experimental results
427 and constitutive modeling. *Canadian Geotechnical Journal*, 44(8), 942-956.
- 428 Artidteang, S., Bergado, D.T., Saowapakpiboon, J., Teerachaikulpanich, N. & Kumar, A.
429 (2011). Enhancement of efficiency of prefabricated vertical drains using surcharge,
430 vacuum and heat preloading, *Geosynthetics International*, 18(1), 35–47.

- 1
2
3 431 Bai, B., Guo, L., & Han, S. (2014). Pore pressure and consolidation of saturated silty clay
4
5 432 induced by progressively heating/cooling. *Mechanics of Materials*, 75, 84-94.
6
7 433 Baldi, G., Hueckel, T., & Pellegrini, R. (1988). Thermal volume changes of the mineral–
8
9 434 water system in low-porosity clay soils. *Canadian Geotechnical Journal*, 25(4), 807-
10
11 435 825.
12
13 436 Bergenstahl, L., Gabrielsson, A., & Mulabdic, M. (1994). Changes in soft clay caused by
14
15 437 increases in temperature. *Proc. 13th Int. Conf. on Soil Mech. and Found. Eng.*, New
16
17 438 Delhi, 1637–1641.
18
19 439 Bourne-Webb P.J., Amatya, B, Soga, K., Amis, T., Davidson, C. & Payne, P. (2009). Energy
20
21 440 pile test at Lambert College, London: geotechnical and thermodynamics aspects of
22
23 441 pile response to heat cycles. *Géotechnique*, 59(3), 237-248.
24
25 442 Brandl, H. (2006). Energy foundationthermoother thermo-active ground structures.
26
27 443 *Géotechnique*, 56(2), 81–122
28
29 444 Burghignoli, A., & Desideri, A. (1988). Influenza della temperatura sulla compressibilità
30
31 445 delle argille. In *Convegno del Gruppo Nazionale di Coordinamento per gli Studi di*
32
33 446 *Ingegneria Geotecnica sul tema: Deformazioni dei terreni ed interazione terreno-*
34
35 447 *struttura in condizioni di esercizio*, Monselice, Italy, 5–6 October, Vol. 1, pp. 19–34.
36
37 448 Burghignoli, A., Desideri, A., & Miliziano, S. (2000). A laboratory study on the
38
39 449 thermomechanical behaviour of clayey soils. *Canadian Geotechnical Journal*, 37(4),
40
41 450 764-780.
42
43 451 Campanella, R. G., & Mitchell, J.K. (1968). Influence of temperature variations on soil
44
45 452 behavior. *Journal of Soil Mechanics & Foundations Div.* 94(3), 709-734.
46
47 453 Cekerevac, C. & Laloui, L. (2004). Experimental study of thermal effects on the mechanical
48
49 454 behaviour of a clay, *Int. J. Numer. Anal. Meth. Geomech.*, 28, 209-228.
50
51
52
53
54
55
56
57
58
59
60

- 1
2
3 455 Cekerevac, C., & Laloui, L. (2010). Experimental analysis of the cyclic behaviour of kaolin
4
5 456 at high temperature. *Géotechnique*, 60(8), 651-655.
6
7 457 Cekerevac, C., Laloui, L., & Vulliet, L. (2005). A novel triaxial apparatus for thermo-
8
9 458 mechanical testing of soils. *Geotechnical Testing Journal*, 28(2), 161-170.
10
11 459 Cheng, W., Hong, P.Y., Pereira, J.M., Cui, Y.J., Tang, A.M., Chen, R.P. (2020). Thermo-
12
13 460 elasto-plastic modeling of saturated clays under undrained conditions. *Computers and*
14
15 461 *Geotechnics*, 125(January):103688.
16
17 462 Coccia, C. J. R., & McCartney, J. S. (2016). Thermal volume change of poorly draining soils
18
19 463 II: model development and experimental validation. *Computers and Geotechnics*, 80,
20
21 464 16-25.
22
23 465 Cui, Y. J., Sultan, N., & Delage, P. (2000). A thermomechanical model for saturated
24
25 466 clays. *Canadian Geotechnical Journal*, 37(3), 607-620.
26
27 467 De Bruyn, D., & Thimus, J. F. (1996). The influence of temperature on mechanical
28
29 468 characteristics of Boom clay: the results of an initial laboratory
30
31 469 programme. *Engineering Geology*, 41(1-4), 117-126.
32
33 470 Delage, P., Sultan, N., & Cui, Y. J. (2000). On the thermal consolidation of Boom
34
35 471 clay. *Canadian Geotechnical Journal*, 37(2), 343-354.
36
37 472 Di Donna and Laloui, L. (2015). Response of soil subjected to thermal cyclic loading:
38
39 473 Experimental and constitutive study, *Engineering Geology*, 190, 65-76.
40
41 474 François, B., & Laloui, L. (2008). ACMEG-TS: A constitutive model for unsaturated soils
42
43 475 under non-isothermal conditions. *International Journal for Numerical and Analytical*
44
45 476 *Methods in Geomechanics*, 32(16), 1955-1988.
46
47 477 Ghaaowd, I. & McCartney, J.S. (2018). Centrifuge modeling of temperature effects on the
48
49 478 pullout capacity of energy piles in clay. *Proc. DFI 43rd Annual Conference on Deep*
50
51 479 *Foundations*. Anaheim, CA. Oct 24-27. 1-7.
52
53
54
55
56
57
58
59
60

- 1
2
3 480 Ghaaowd, I., McCartney, J.S., Huang, X., Saboya, F., & Tibana, S. (2018). Issues with
4
5 481 centrifuge modeling of energy piles in soft clays. *Proc. 9th International Conference*
6
7 482 *on Physical Modeling in Geotechnics: Physical Modelling in Geotechnics*. A.
8
9 483 McNamara et al., eds. Taylor & Francis Group, London. 1365-1370.
10
11
12 484 Ghaaowd, I. and McCartney, J.S. (2021). Centrifuge modeling methodology for energy pile
13
14 485 pullout from saturated soft clay. *Geotechnical Testing Journal*. 45(2), 332-354.
15
16
17 486 Goode, J.C., & McCartney, J.S. (2015). Centrifuge modeling of boundary restraint effects in
18
19 487 energy foundations. *Journal of Geotechnical and Geoenvironmental Engineering*.
20
21 488 141(8), 04015034.
22
23
24 489 Graham, J., Tanaka, N., Crilly, T., & Alfaro, M. (2001). Modified Cam-Clay modelling of
25
26 490 temperature effects in clays. *Canadian Geotechnical Journal*, 38(3), 608-621.
27
28
29 491 Hamidi, A., Tourchi, S., & Kardooni, F. (2017). A critical state based thermo-elasto-plastic
30
31 492 constitutive model for structured clays. *Journal of Rock Mechanics and Geotechnical*
32
33 493 *Engineering*, 9(6), 1094-1103.
34
35
36 494 Hong, P.Y., Pereira, J.M., Tang, A.M., & Cui, Y.J. (2013). On some advanced thermo-
37
38 495 mechanical models for saturated clays. *International Journal for Numerical and*
39
40 496 *Analytical Methods in Geomechanics*, 37(17), 2952-2971.
41
42
43 497 Hong, P.Y., Pereira, J.M., Cui, Y.J., & Tang, A.M. (2016). A two-surface thermo-mechanical
44
45 498 model for saturated clays. *Int. J. Numer. Anal. Meth. Geomech.* 40(7), 1059–1080.
46
47
48 499 Houston, S. L., Houston, W. N., & Williams, N. D. (1985). Thermo-mechanical behavior of
49
50 500 seafloor sediments. *Journal of Geotechnical Engineering*, 111(11), 1249-1263.
51
52
53 501 Hueckel, T., & Baldi, G. (1990). Thermoplasticity of saturated clays: experimental
54
55 502 constitutive study. *Journal of Geotechnical Engineering*, 116(12), 1778-1796.
56
57
58 503 Hueckel, T., François, B., & Laloui, L. (2011). Temperature-dependent internal friction of
59
60 504 clay in a cylindrical heat source problem. *Géotechnique*, 61(10), 831-844.

- 1
2
3 505 Jaradat, K.A., & Abdelaziz, S.L. (2019). Thermomechanical triaxial cell for rate-controlled
4
5 506 heating-cooling cycles. 43(4), DOI: 10.1520/GTJ20180354.
6
7 507 Kuntiwattanakul, P., Towhata, I., Ohishi, K., & Seko, I. (1995). Temperature effects on
8
9 508 undrained shear characteristics of clay. *Soils and Foundations*, 35(1), 147-162.
10
11 509 Laloui, L., & Cekerevac, C. (2003). Thermo-plasticity of clays: an isotropic yield
12
13 510 mechanism. *Computers and Geotechnics*, 30(8), 649-660.
14
15 511 Laloui, L., & François, B. (2009). ACMEG-T: soil thermoplasticity model. *Journal of*
16
17 512 *Engineering Mechanics*, 135(9), 932-944.
18
19 513 Laloui, L., Nuth, M. & Vulliet, L. (2006). Experimental and numerical investigation of the
20
21 514 behavior of a heat exchanger pile. *International Journal for Numerical and Analytical*
22
23 515 *Methods in Geomechanics*, 30(8), 763-781
24
25 516 Laloui, L., Olgun, C. G., Sutman, M., McCartney, J. S., Coccia, C. J., Abuel-Naga, H. M. &
26
27 517 Bowers, G. A. (2014). Issues involved with thermoactive geotechnical systems:
28
29 518 Characterization of thermomechanical soil behavior and soil-structure interface
30
31 519 behavior. *DFI Journal-The Journal of the Deep Foundations Institute*, 8(2), 108-
32
33 520 120.Li, Y., Dijkstra, J., & Karstunen, M. (2018). Thermomechanical creep in sensitive
34
35 521 clays. *Journal of Geotechnical and Geoenvironmental Engineering*, 144(11),
36
37 522 04018085.
38
39 523 Lingnau, B. E., Graham, J., Yarechewski, D., Tanaka, N., & Gray, M. N. (1996). Effects of
40
41 524 temperature on strength and compressibility of sand-bentonite buffer. *Engineering*
42
43 525 *Geology*, 41(1-4), 103-115.
44
45 526 McCartney, J.S. & Murphy, K.D. (2017). Investigation of potential dragdown/uplift effects
46
47 527 on energy piles. *Geomechanics for Energy and the Environment*. 10(June), 21-28.
48
49 528 Ng, C.W.W., Shi, C., Gunawan, A., & Laloui, L. (2014). Centrifuge modelling of energy
50
51 529 piles subjected to heating and cooling cycles in clay. *Géotech. Lett.* 4(4), 310–316.
52
53
54
55
56
57
58
59
60

- 1
2
3 530 Ng, C.W.W., Farivar, A., Gomaa, S.M.M.H., & Jafarzadeh, F. (2021). Centrifuge modeling
4
5 531 of cyclic nonsymmetrical thermally loaded energy pile groups in clay. *Journal of*
6
7 532 *Geotechnical and Geoenvironmental Engineering*, 147(12), 04021146.
- 8
9
10 533 Salager, C., Bergado, D.T. & Abuel-Naga, H.M. (2010). Full-scale embankment
11
12 534 consolidation test using prefabricated vertical thermal drains. *Soils and Foundations*,
13
14 535 50(5), 599-608.
- 15
16
17 536 Salager, S., Laloui, L. & Nuth, M. (2012). Efficiency of thermal vertical drains for the
18
19 537 consolidation of soils. *2nd Int. Conf. on Transportation Geotechnics*, Hokaido. 1-10.
- 20
21 538 Plum, R. L., Esrig, M. I. (1969). Some temperature effects on soil compressibility and pore
22
23 539 water pressure. *Nat. Acad. Sci. Res. Council. Res. Board, Rep 103*. (10), 231-242.
- 24
25
26 540 Rotta Loria, A.F. and Coulibaly, J.B. (2021). Thermally induced deformation of soils: A
27
28 541 critical overview of phenomena, challenges and opportunities, *Geomechanics for*
29
30 542 *Energy and the Environment*. 25, 100193.
- 31
32
33 543 Samarakoon, R., Ghaaowd, I. & McCartney, J.S. (2018). Impact of drained heating and
34
35 544 cooling on undrained shear strength of normally consolidated clay. *Proceedings of the*
36
37 545 *2nd International Symposium on Energy Geotechnics*. Lausanne, Switzerland. Sep.
38
39 546 26-28. A. Ferrari, L. Laloui, eds. Springer, Vienna. 243-249.
- 40
41
42 547 Samarakoon, R. & McCartney, J.S. (2020). Effect of Drained Heating and Cooling on the
43
44 548 Preconsolidation Stress of Saturated Normally Consolidated Clays. *Proc. Geo-*
45
46 549 *Congress 2020*. GSP 315, ASCE, Reston, VA. 620-629.
- 47
48
49 550 Shibasaki, T., Matsuura, S., & Hasegawa, Y. (2017). Temperature-dependent residual shear
50
51 551 strength characteristics of smectite-bearing landslide soils. *Journal of Geophysical*
52
53 552 *Research: Solid Earth*, 122(2), 1449-1469.
- 54
55
56 553 Taylor, D. W. (1942). *Research on Consolidation of Clays*. Massachusetts Institute of
57
58 554 Technology, Department of Civil and Sanitary Engineering, Serial No. 82, 1.
59
60

- 1
2
3 555 Towhata I, Kuntiwattanakul P, Seko I, & Ohishi K. (1993). Volume change of clays induced
4
5 556 by heating as observed in consolidation tests. *Soils and Foundations*, 33(4), 170–83.
6
7 557 Tsutsumi A, & Tanaka H. (2012). Combined effects of strain rate and temperature on
8
9 558 consolidation behavior of clayey soils. *Soils and Foundations*, 52(2), 207–15.
10
11 559 Uchaipichat, A., & Khalili, N. (2009). Experimental investigation of thermo-hydro-
12
13 560 mechanical behaviour of an unsaturated silt. *Géotechnique*, 59(4), 339-353.
14
15 561 Vega, A. & McCartney, J.S. (2015). Cyclic heating effects on thermal volume change of silt.
16
17 562 *Environmental Geotechnics*. 2(5), 257-268.
18
19 563 Vryzas, Z., Kelessidis, V.C., Nalbantian, L., Zaspalis, V., Gerogiorgis, D.I., &
20
21 564 Wubulikasimu, Y. (2017). Effect of temperature on the rheological properties of neat
22
23 565 aqueous Wyoming sodium bentonite dispersions. *Applied Clay Science*, 136, 26-36.
24
25 566 Yazdani, S., Helwany, S., & Olgun, G. (2019a). Influence of temperature on soil–pile
26
27 567 interface shear strength. *Geomechanics for Energy and the Environment*, 18, 69-78.
28
29 568 Yazdani S., Helwany S., & Olgun G. (2019b). Investigation of thermal loading effects on
30
31 569 shaft resistance of energy pile using laboratory-scale model. *Journal of Geotechnical*
32
33 570 *and Geoenvironmental Engineering*, 145(9): 04019043.
34
35 571 Yazdani S., Helwany S., & Olgun G. (2021). The mechanisms underlying long-term shaft
36
37 572 resistance enhancement of energy piles in clays. *Canadian Geotechnical Journal*. 58,
38
39 573 1640-1653. Zeinali, S.M. & Abdelaziz, S.L. (2021). Thermal consolidation theory.
40
41 574 *Journal of Geotechnical and Geoenvironmental Engineering*. 147(1), 04020147.
42
43 575 Zhou, C. & Ng, C.W.W. (2018). A new thermo-mechanical model for structured soil.
44
45 576 *Géotechnique*, 68(12), 1751-7656.
46
47
48
49
50
51
52
53
54
55
56
57
58
59
60

577 **TABLE 1. Summary of conclusions regarding the influence of temperature on shear strength.**

Reference	Soil type	Condition	Type of heating	Type of shear	Remarks
Houston <i>et al.</i> (1985)	Ocean sediments (illites and smectites).	NC	U	CIU	Undrained shear strength increased when drained thermal consolidation took place at high temperatures.
Hueckel & Baldi (1990)	Boom clays and one clay slime.	OC	D	CID	Shear strength declined in both cases.
Lingnau <i>et al.</i> (1996)	Mixture of silica sand and sodium bentonite.	NC	D	CIU, CID	Strength is independent of temperature.
De Bruyn & Thimus (1996)	Boom Clay	NC	D	CIU	Decrease in strength due to the decline in friction angle and a slight rise in apparent cohesion.
Kuntiwattanakul <i>et al.</i> (1995)	Kaolin clay	NC, OC	D	CIU	Increase strength in NC but it is not observed for OC soils
Graham <i>et al.</i> (2001)	Reconstituted illite	OC	D, U	CID	The critical state line is independent of temperature.
Burghignoli <i>et al.</i> (2000)	Reconstituted and natural clay	NC	D, U	CIU	Strength is independent of temperature.
Cekerevac <i>et al.</i> (2005)	Kaolin	OC	D	CID	Shear strength increased only for NC conditions.
Abuel-Naga <i>et al.</i> (2007a)	Soft clay (LL=103%)	NC, OC	D	CID and CIU	Shear strength increased for both cases, NC and OC.
Uchaipichat & Khalili (2009)	Silt	NC, OC	U	Suction Controlled CD	Peak shear strength decreased but at critical state condition there was no temperature effect
Shibasaki <i>et al.</i> (2017)	Smectite	NC	D	CD - Direct shear	Shear strength increased.
Samarakoon <i>et al.</i> (2018)	Kaolinite	NC	U	CIU	Higher strength after thermal consolidation with even higher strength after subsequent cooling before shearing.

578 D = Drained, U=Undrained, OC=Overconsolidated, NC=Normally Consolidated

TABLE 2. Physical properties of natural marine clay.

<i>Parameter</i>	<i>Value</i>
gravimetric water content (w) "after homogenization (%)"	91.2
Liquid limit (LL)	106
Plastic limit (PL)	41
Plasticity index (PI)	65
Specific gravity (G_s)	2.69

For Review Only

TABLE 3. Total number of tests and their respective characteristics.

<i>Test</i>	<i>Effective confining stress (kPa)</i>	<i>OCR</i>	<i>Thermal consolidation temperature (°C)</i>	<i>Shearing temperature (°C)</i>
S1	100	1		
S2	200	1		
S3	400	1	23 (none)	23
S4	50	4		
S6	100	1		
S7	200	1	40	
S8	400	1		23
S9	100	1		
S10	200	1	55	
S11	400	1		

TABLE 4. Initial and final physical properties of the specimens.

<i>Test</i>	w_i (%)	e_o	w_f (%)	e_{f1}	e_{f2}	e_{f3}
S1	70.63	1.90	55.02	1.48	-	-
S2	73.23	1.97	50.19	1.35	-	-
S3	71.00	1.91	41.26	1.11	-	-
S6	70.63	1.90	54.65	1.48	1.45	1.47
S7	73.23	1.97	49.81	1.36	1.32	1.34
S8	73.61	1.98	40.89	1.14	1.09	1.10
S9	71.38	1.92	53.90	1.50	1.42	1.45
S10	69.89	1.88	46.10	1.29	1.20	1.24
S11	70.26	1.89	39.03	1.09	1.01	1.05

w_i = initial gravimetric water content

w_f = final gravimetric water content (after cooling when applied)

e_o = initial void ratio

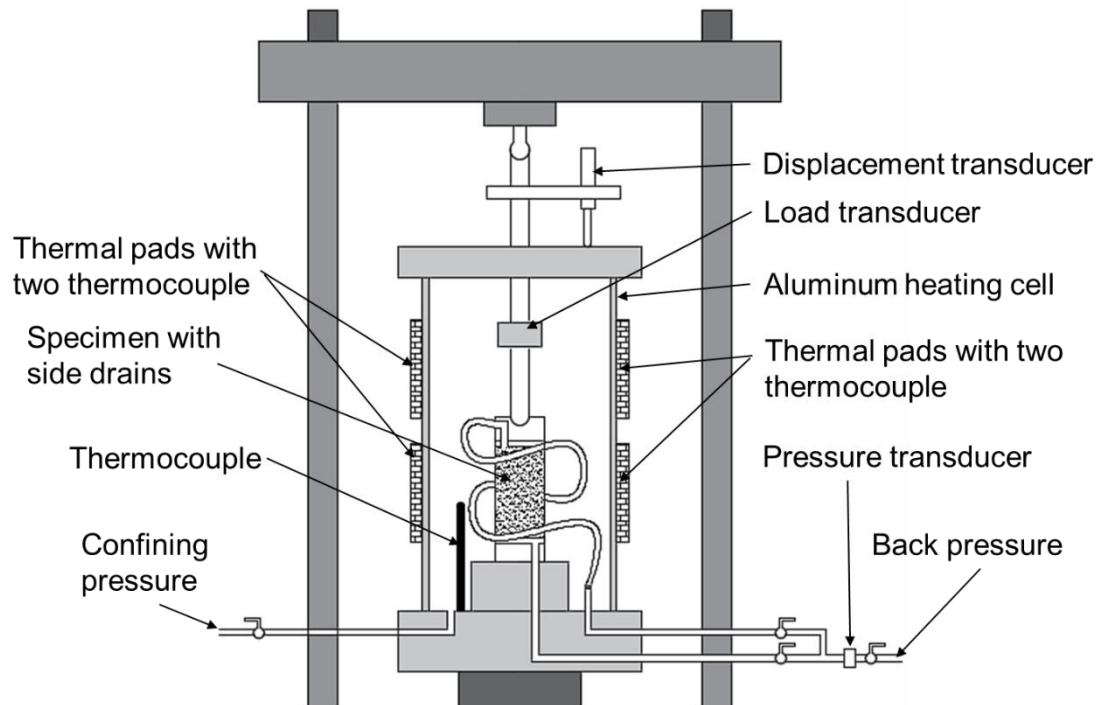
TABLE 5. Equivalent effective mean initial stress p'_{ieq} by using the Cam-Clay approach.

p'_i	55°C	40°C	Cam Clay	23°C	40°C	55°C	p'_{ieq}	
kPa	e_{f3}		s_u (Eq 1)	s_u -triaxial			40°C	55°C
100	1.45	1.48	32.0	35.0	82.0	90	255.90	280.86
200	1.29	1.36	64.0	67.0	150.0	165	468.10	514.91
400	1.09	1.14	128.2	158.0	285.0	300	889.39	936.20

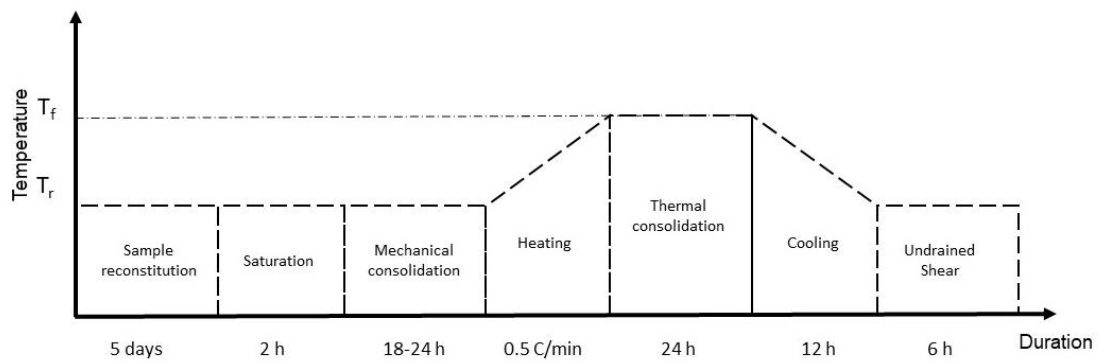
p'_{ieq} = Initial confining effective stress necessary to provide the same s_u obtained by triaxial tests. Strength and stress in kPa.

For Review Only

Figure 1. Schematic of the thermal triaxial cell.



View Only

Figure 2. Procedure used for CIU thermal triaxial tests.

For Review Only

Figure 3. Void ratio variation during thermal consolidation for S6, S7 and S8 tests

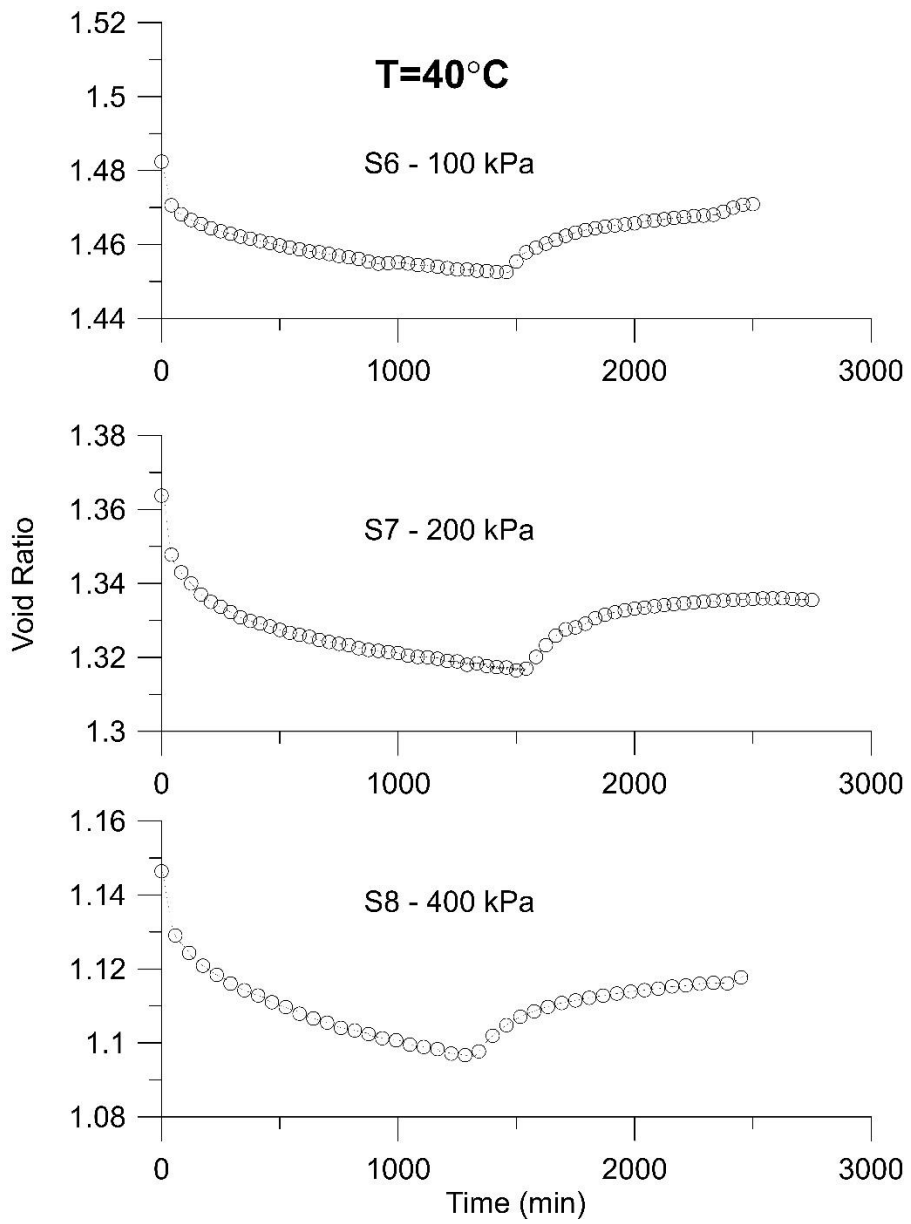


Figure 4. Transient evolution in volumetric thermal strains after heating to 40°C and 55°C.

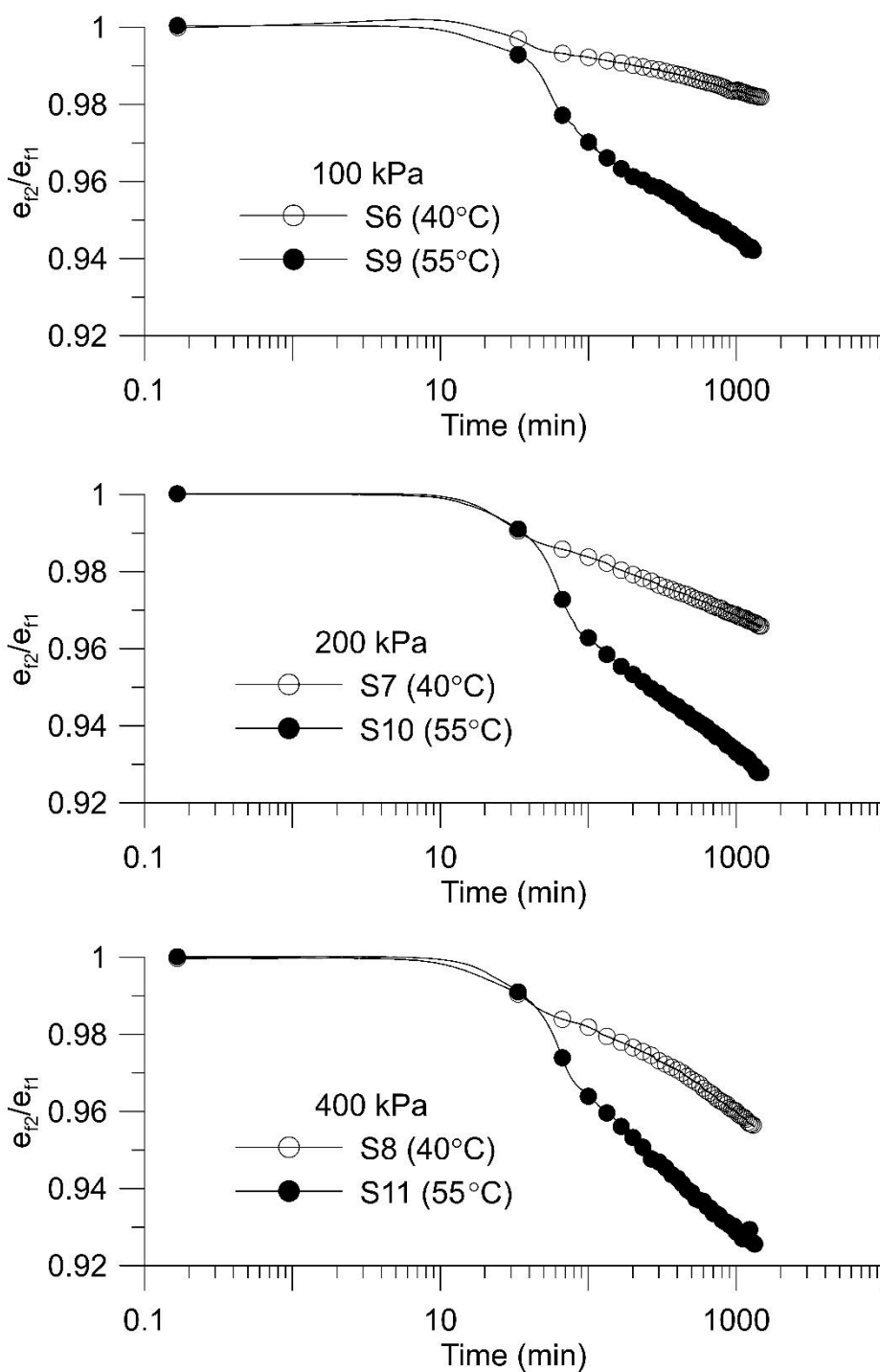
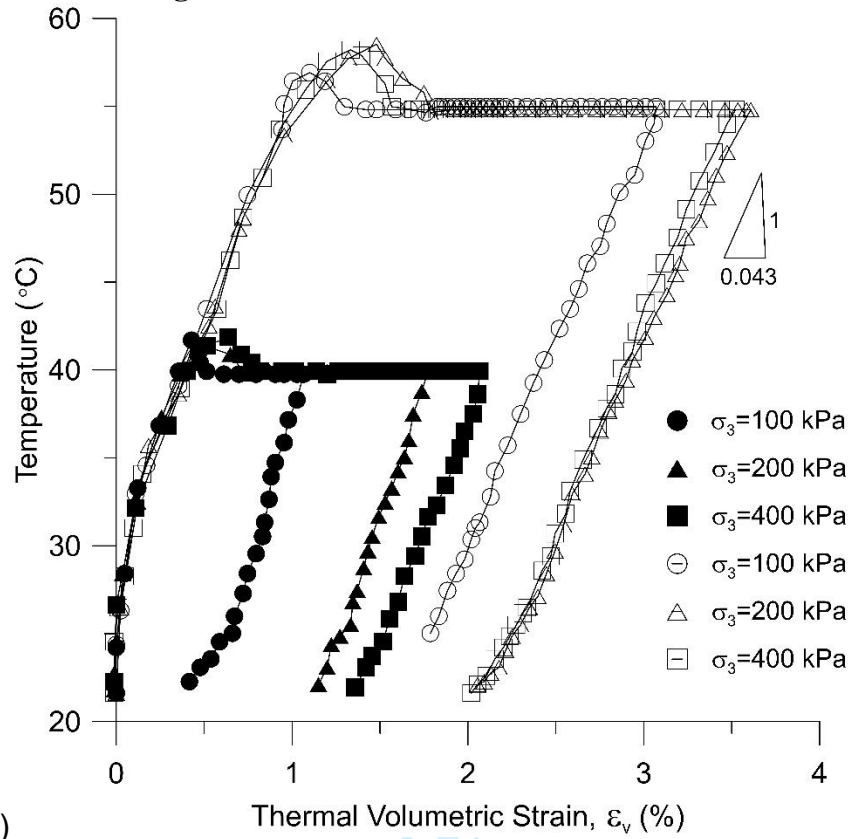
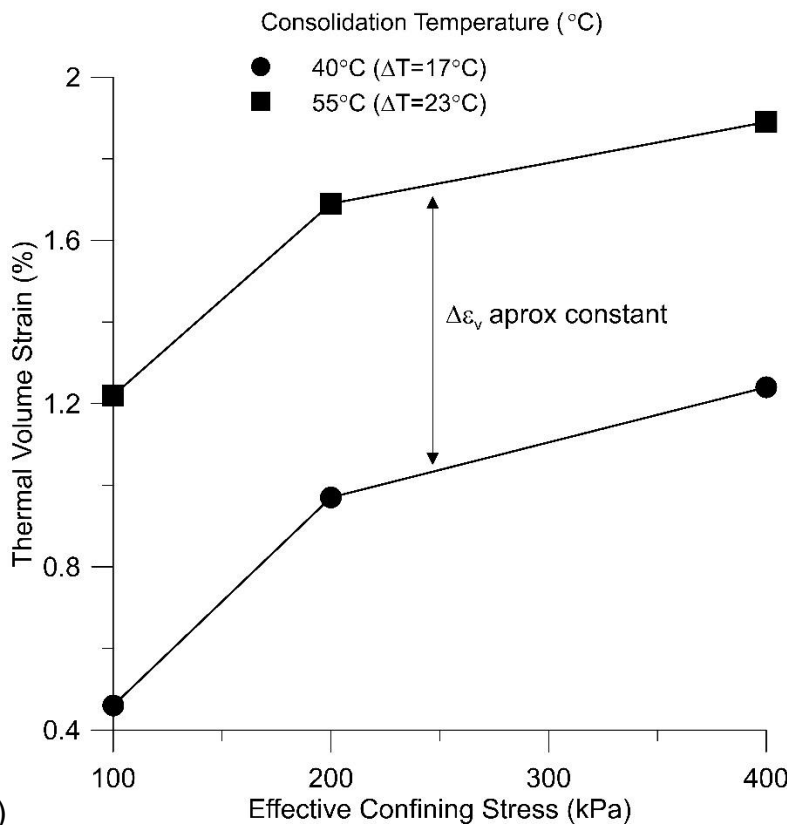


Figure 5. (a) Thermal volumetric deformation (ϵ_v) vs. temperature (T) curves of the thermal triaxial tests at 40°C and 55°C. (b) Thermal volume change under constant temperature and confining stress.



(a)



(b)

Figure 6. Deviator stress vs. axial strain (σ_a vs. ϵ_1); (a) and pore pressure vs. axial strain (Δu vs. ϵ_1) Tests S1 to S3 (references); (b) S6 to S8 (thermal consolidated at 40°C); (c) S9 to S11 (thermal consolidated at 55°C).

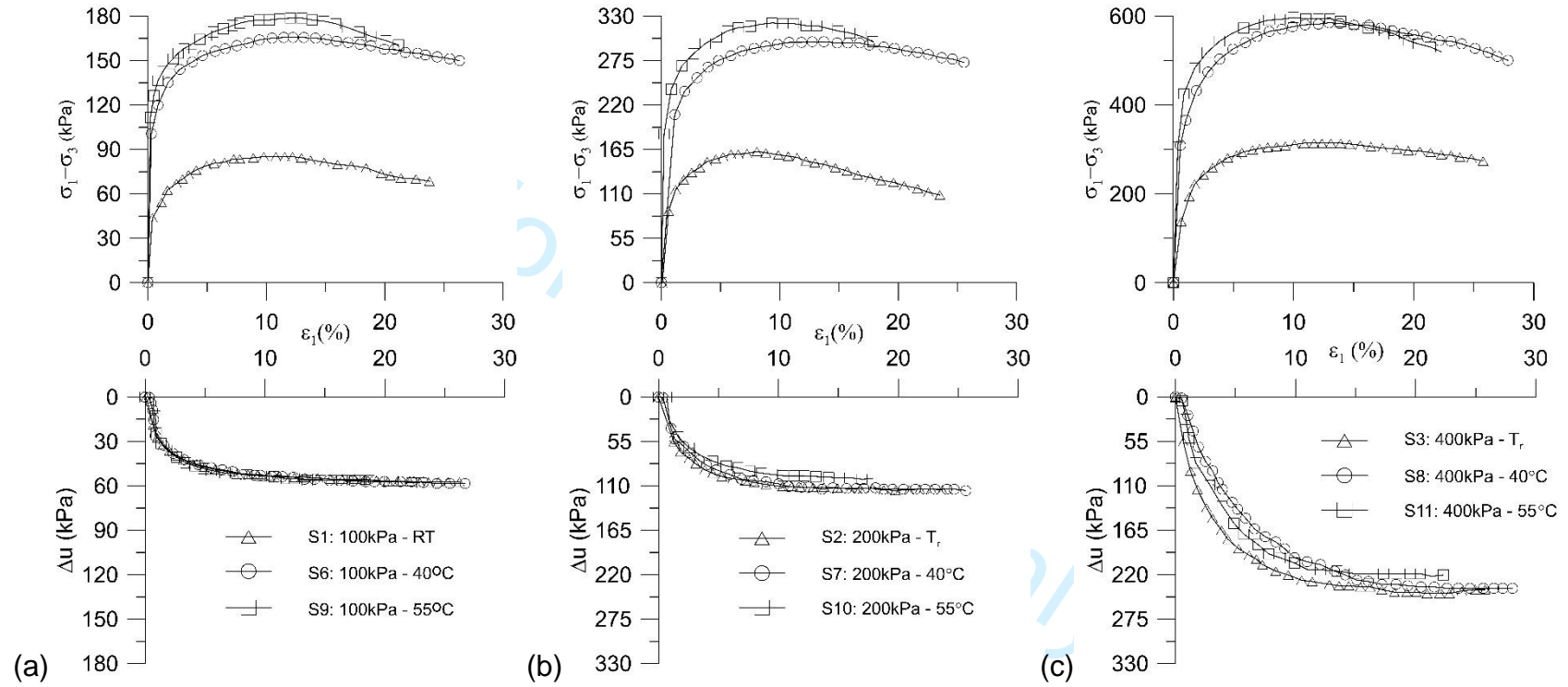


Figure 7. (a) Effective stress paths (ESP), (b) LIC and CSL in the compression plane and (c) equivalent time compression line in $\ln p'$ vs. vol. strain in the compression plane for conventional and thermal triaxial tests

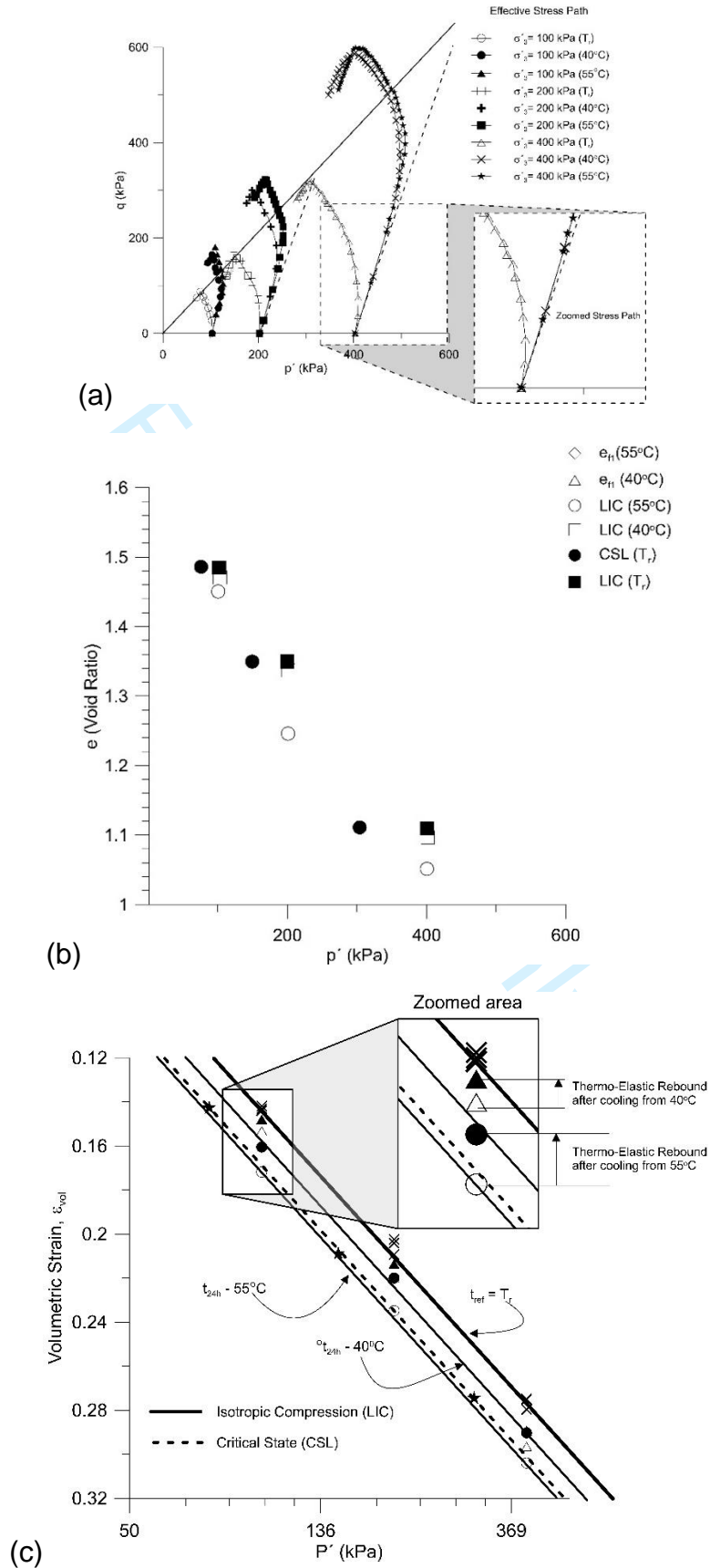


Figure 8. Changes in undrained peak shear strength with thermal consolidation.

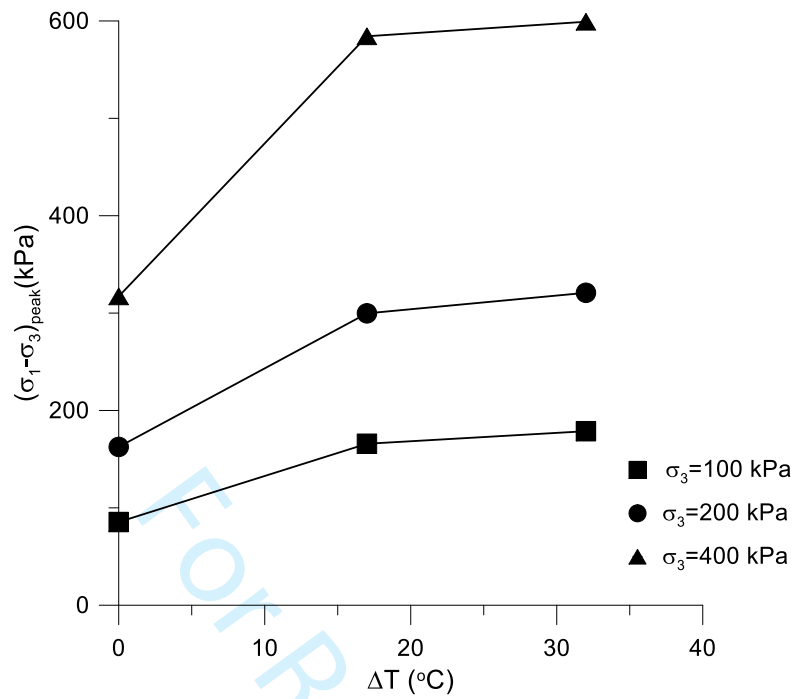


Figure 9. Young's modulus defined at 1% axial strain for tests at different confining stresses and temperatures.

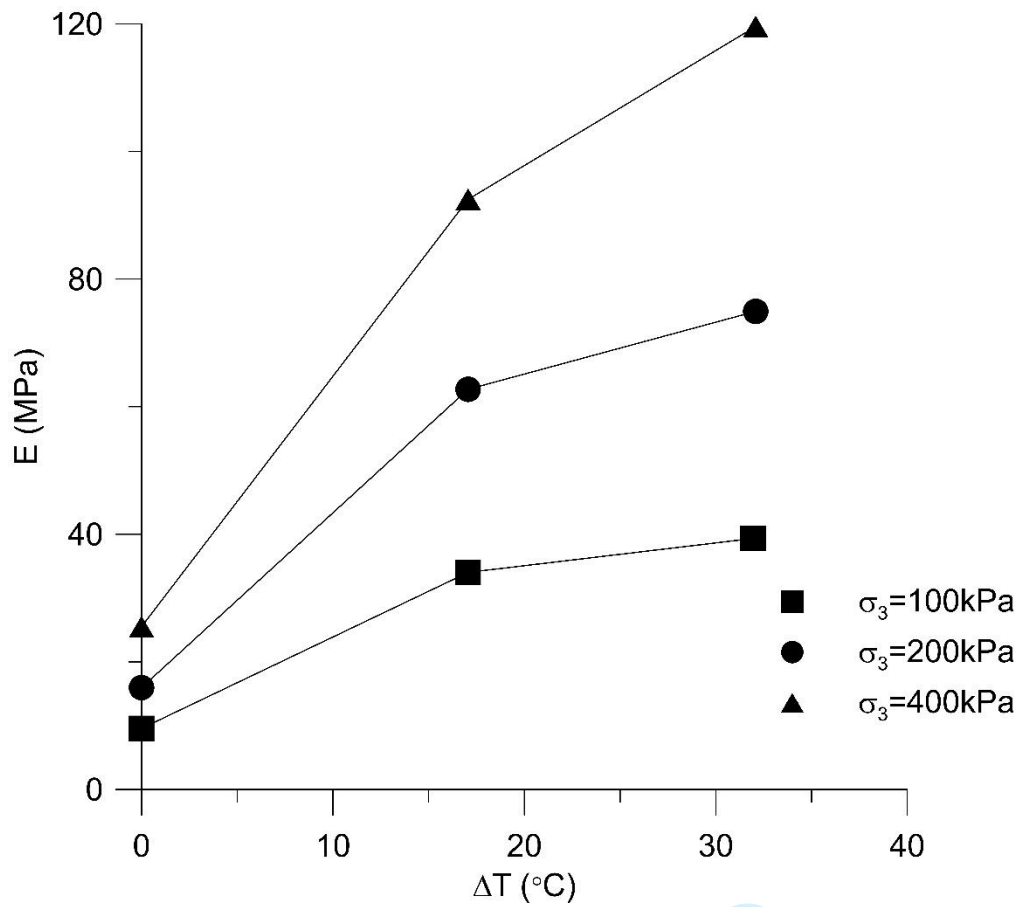


Figure 10. Equivalent or pseudo consolidation effective stress (p'_{ct}) generated by thermal cycle up to 55°C.

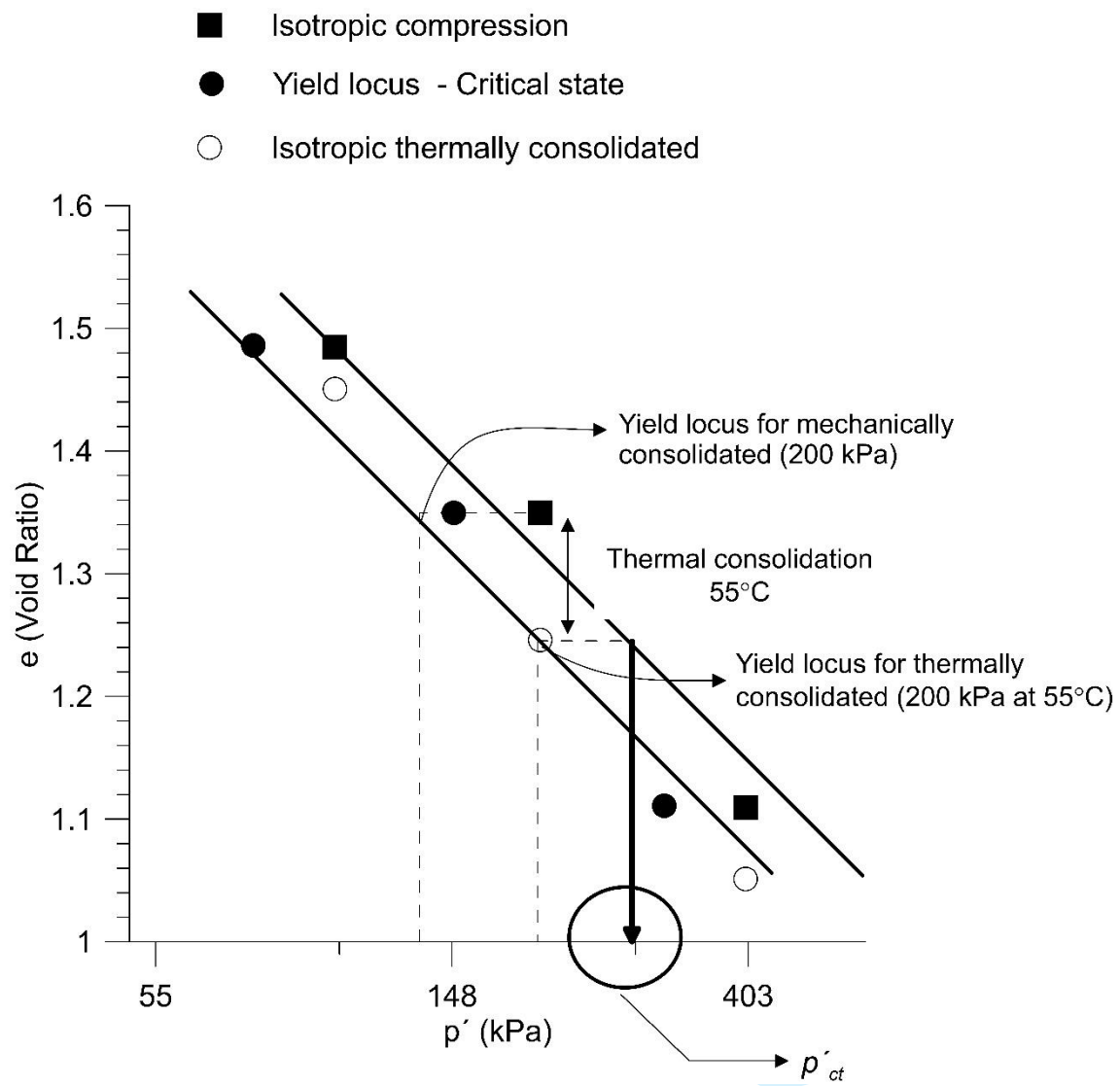


Figure 11. Effective stress paths for thermal triaxial tests at 55°C with the thermal equivalent pre-consolidation effective stress " p'_{ct} ".

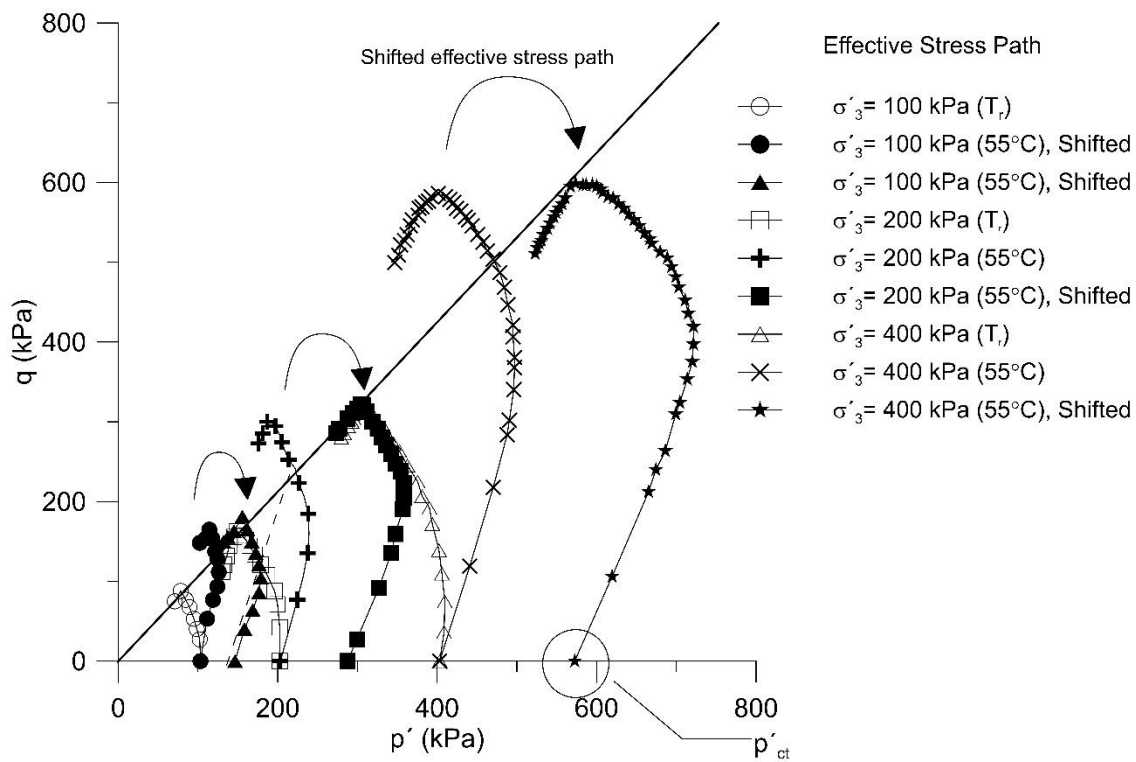


Figure 12. Cam-Clay effective stress path and observed shifted effective stress path

